



**HAL**  
open science

## Impact of Molecular Weight on Anti-Bioadhesion Efficiency of PDMS-Based Coatings

Mama Aïssata Bangoura, David Mimeau, Eric Balnois, Karine Réhel, Fabrice Azemar, Isabelle Linossier

► **To cite this version:**

Mama Aïssata Bangoura, David Mimeau, Eric Balnois, Karine Réhel, Fabrice Azemar, et al.. Impact of Molecular Weight on Anti-Bioadhesion Efficiency of PDMS-Based Coatings. *Coatings*, 2024, 14 (1), pp.149. 10.3390/coatings14010149 . hal-04827827

**HAL Id: hal-04827827**

**<https://hal.science/hal-04827827v1>**

Submitted on 10 Dec 2024

**HAL** is a multi-disciplinary open access archive for the deposit and dissemination of scientific research documents, whether they are published or not. The documents may come from teaching and research institutions in France or abroad, or from public or private research centers.



L'archive ouverte pluridisciplinaire **HAL**, est destinée au dépôt et à la diffusion de documents scientifiques de niveau recherche, publiés ou non, émanant des établissements d'enseignement et de recherche français ou étrangers, des laboratoires publics ou privés.



Distributed under a Creative Commons Attribution 4.0 International License

## Article

# Impact of Molecular Weight on Anti-Bioadhesion Efficiency of PDMS-Based Coatings

Mama Aïssata Bangoura <sup>1,\*</sup>, David Mimeau <sup>2</sup>, Eric Balnois <sup>3</sup>, Karine Réhel <sup>1</sup>, Fabrice Azemar <sup>1</sup>  
and Isabelle Linossier <sup>1</sup>

<sup>1</sup> Laboratoire de Biotechnologie et de Chimie Marines (LBCM), EMR CNRS 6076, Université Bretagne Sud, IUEM, CS7030, 56321 Lorient, France; karine.rehel@univ-ubs.fr (K.R.); fabrice.azemar@univ-ubs.fr (F.A.); isabelle.linossier@univ-ubs.fr (I.L.)

<sup>2</sup> Nautix, Parc d'activités Les 5 Chemins, 56520 Guidel, France; d.mimeau@nautix.com

<sup>3</sup> Laboratoire de Biotechnologie et de Chimie Marines (LBCM), EMR CNRS 6076, Université de Bretagne Occidentale, 29000 Quimper, France; eric.balnois@univ-brest.fr

\* Correspondence: mama-aissata.bangoura@univ-ubs.fr

**Abstract:** Silicone elastomer coatings have shown successful fouling release ability in recent years. To further enhance the design of silicone coatings, it is necessary to fully understand the mechanisms that contribute to their performance. The objective of this study was to examine the relationship between the molecular weight of polydimethylsiloxane (PDMS) and antibioadhesion efficiency. PDMS-based coatings were prepared via a condensation reaction, with a controlled molecular weight ranging from 0.8 to 10 kg·mol<sup>-1</sup>. To evaluate changes in surface wettability and morphology, contact angle experiments and atomic force microscopy (AFM) were performed. Finally, the antibioadhesion and self-cleaning performance of PDMS coatings was carried out during *in situ* immersion in Lorient harbor for 12 months. Despite small variations in surface properties depending on the molecular weight, strong differences in the antibioadhesion performance were observed. According to the results, the best antibioadhesion efficiency was obtained for coatings with an Mn between 2 and 4 kg·mol<sup>-1</sup> after 12 months. This paper provides for the first time the impact of the molecular weight of PDMS on antibioadhesion efficiency in a real marine environment.

**Keywords:** silicone elastomers; anti-bioadhesion; polydimethylsiloxane; fouling release coating; self-condensation



**Citation:** Bangoura, M.A.; Mimeau, D.; Balnois, E.; Réhel, K.; Azemar, F.; Linossier, I. Impact of Molecular Weight on Anti-Bioadhesion Efficiency of PDMS-Based Coatings. *Coatings* **2024**, *14*, 149. <https://doi.org/10.3390/coatings14010149>

Academic Editor: Giancarlo Galli

Received: 21 December 2023

Revised: 11 January 2024

Accepted: 18 January 2024

Published: 21 January 2024



**Copyright:** © 2024 by the authors. Licensee MDPI, Basel, Switzerland. This article is an open access article distributed under the terms and conditions of the Creative Commons Attribution (CC BY) license (<https://creativecommons.org/licenses/by/4.0/>).

## 1. Introduction

Marine biofouling, the accumulation of marine organisms such as bacteria, algae, and barnacles on immersed surfaces, is a major problem for the naval industry, generating severe economic and ecological impacts. Biofouling of ship hulls induces increased fuel consumption, an important loss of vessel maneuverability, and expensive maintenance costs [1–3]. In addition, marine biofouling leads to the introduction of invasive marine species in non-native environments through ship transport. Antifouling paints are widely used to control bioadhesion via the use of biocidal molecules. However, these kinds of coatings are highly regulated to protect marine environments, hence new strategies with a lower environmental impact are required.

More recent research in the field has seen the emergence of technologies without biocides, known as fouling-release coatings (FRC). Silicone elastomer coatings such as polydimethylsiloxane (PDMS) have shown successful antibioadhesion properties when subjected to hydrodynamic forces such as those produced by movement in water. PDMS is one of the most widely used soft polymers due to specific properties: high flexibility, biocompatibility, elasticity, and high availability. Its antibioadhesion efficiency has been attributed to three main characteristics: an optimal critical surface energy to minimize adhesion forces [4], a low elastic modulus, and a low roughness to facilitate the detachment

of hard foulants such as barnacles [5,6] under shear forces during navigation. Silicone-based coatings are generally prepared via a hydrosilylation reaction or a condensation reaction [7]. Hydrosilylation describes the addition reactions between two types of PDMS, one containing vinyl groups and the other silane groups, in the presence of a platinum-based catalyst [8]. On the other hand, a silicone crosslinker with many alkoxy silane groups, and a polysiloxane precursor with silanol end-groups can undergo a condensation reaction [9].

The first use of crosslinked silicone to prevent the adhesion of barnacles was patented by Robbart Edward in 1961 [10]. He pointed out that siloxane polymers such as methyl polydimethylsiloxane, methyl phenyl polydimethylsiloxane, and ethyl polydimethylsiloxane were particularly suitable for silicone coatings. He had already claimed that the efficiency of silicon resins in preventing the accumulation of marine organisms could be at least related to the smoothness of the silicone surface. Many studies have reported on the efficiency of silicone coatings. Truby et al. showed that the incorporation of free polydimethyldiphenylsiloxane (PDMDPS) oil in a cured polydimethylsiloxane (PDMS) network decreased the adhesion of barnacles and certain species of oysters [11]. Wynne et al. carried out a study to compare the fouling-release performance of filled condensation-cured room-temperature vulcanizing (RTV) silicone rubber coatings [9,12] with that of an unfilled hydrosilylation system (with the same molecular weight of PDMS macromonomers). They demonstrated that all hydrosilylation-cured coatings released barnacles (*Balanus eburneus*) more readily than filled RTV. The surface roughness observed for filled RTV may certainly improve the adhesion of foulants [9]. In addition, Stein et al. have tried to fully understand the effect of the filler (coating composition) of both condensation-cured and hydrosilylation-cured silicone coatings on barnacle attachment strength. They showed that barnacle adhesion increased as the filler loading increased in both systems [13]. They also tried to understand the relationship between the molecular architecture (crosslinking density) and the adhesion of barnacles in hydrosilylation-cured systems. They observed no significant effect of the crosslinking density on the adhesion strength of barnacles, but some change on the failure mechanism of barnacles were noticed. They have suggested that lower crosslink density was better for stable (durable) coating. In another study, the influence of the elastic modulus on the release of the soft foulant alga (*Ulva linza*) from hydrosilylated PDMS coating has been investigated. No significant effect of elastic moduli ranging from 0.2 to 9.4 MPa was observed for the settlement of *Ulva* sp. zoospores. However, more detachment of sporeling was observed for the softer materials with lower moduli (0.2 and 0.8 MPa): the sporeling were readily detached on these coatings [5]. In another study, Gray et al. showed that the settlement of larvae could be positively correlated with elastic modulus [14].

The literature states that several specific parameters can contribute to the antibioadhesion performance of silicone-based coatings. We identified molecular weight as one of these parameters. To date, few studies have reported the relationship between the network characteristics of PDMS coatings and their antibioadhesion performances. In particular, there is a need to examine the impact of molecular weight on efficiency. Most of these studies were performed on silicone coatings obtained via hydrosilylation. In this work, the focus was on condensation reactions. The successive mechanism of alkoxy silane hydrolysis and condensation reactions enable the formation, by aggregation, of a three-dimensional network at room temperature. The material thus formed presents intermolecular chemical bonds ensuring the mechanical cohesion of the material. To study the relationship between chain size and antibioadhesion efficiency, different PDMS-based coatings were prepared via condensation reaction, with a controlled molecular weight ranging from 0.8 to 10 kg·mol<sup>-1</sup>. In contrast with other methods usually used, the PDMS coatings studied were obtained via self-condensation without a precursor, in the presence of a catalyst at room temperature. Indeed, PDMS used in this study were modified using thiol-ene click chemistry to obtain crosslinkable methoxysilane end groups. In the presence of humidity and a catalyst, a tridimensional network could be formed [15]. The polymeric solutions obtained were applied on different surfaces to be characterized after curing. The Soxhlet extraction method was

employed to study crosslinking efficiency. The key properties for fouling release such as surface roughness and elastic modulus were studied with atomic force microscopy (AFM), and surface energy was calculated using contact angle measurements. Finally, the influence of molecular weight on the antibioadhesion of PDMS coatings was investigated during the immersion of samples in the Atlantic Ocean (Lorient harbor) in static conditions for 12 months.

## 2. Materials and Methods

### 2.1. Materials

Three vinyl-terminated polydimethylsiloxanes (Mn: 800 g·mol<sup>-1</sup>, PDMS-V0.8K; Mn: 6000 g·mol<sup>-1</sup>, PDMS-V6K; Mn: 9400 g·mol<sup>-1</sup>, PDMS-V10K) were acquired from Gelest Inc. (Morrisville, NC, USA). Polydimethylsiloxane and bis(3-aminopropyl)-terminated (Mn: 2500 g·mol<sup>-1</sup>, PDMS-N2.5K) were purchased from Sigma Aldrich® (Taufkirchen, Germany). Linear, trimethoxysilane-terminated polydimethylsiloxane (Mn: 4010 g·mol<sup>-1</sup> PDMS-TMS4K) was kindly offered by our industrial partner. The zinc complex catalyst was purchased from King Industries Inc. (Norwalk, CT, USA). The 2,2-dimethoxy-2-phenylacetophenone (>99% DMPA) was purchased from Thermo Fisher Scientific (Waltham, MA, USA). The *N,N'*-dicyclohexylcarbodiimide (>98% DCC), 4-dimethylaminopyridine (>99% DMAP), (3-mercaptopropyl)-trimethoxysilane (>96% HS-TMS), and 4-pentenoic acid were purchased from TCI Chemicals (Zwijndrecht, Belgium). Chloroform, hexane, acetonitrile, toluene, and glass microscope slides (76 mm × 26 mm × 1 mm) were purchased from VWR International (Radnor, PE, USA). Deuterated chloroform (CDCl<sub>3</sub>) for Eurositop <sup>1</sup>H NMR analysis was acquired from (Hadfield, UK). All products were used as received.

### 2.2. PDMS Functionalization

#### 2.2.1. PDMS-NH<sub>2</sub> Functionalization via Steglich Esterification: PDMS-V2.5K

Vinyl-terminated polydimethylsiloxane as PDMS-V2.5K was prepared via Steglich esterification using *N,N'*-dicyclohexylcarbodiimide as a coupling agent, as previously described by Gillet et al. [15]. PDMS-NH<sub>2</sub> (1 g, 1 equiv), pentenoic acid (0.12 g, 4 equiv), *N,N'*-dicyclohexylcarbodiimide (0.38 g, 6 equiv), and 4-dimethylaminopyridine (0.11 g, 3 equiv) were dissolved in anhydrous toluene (Figure 1). Nitrogen was bubbled into the solution for 30 min. The reaction mixture was stirred at 135 °C for 6 h under reflux. The resulting product was cooled to room temperature and filtered to remove solid byproduct. The solvent was then removed under reduced pressure. The colored oil obtained was dissolved in hexane and washed 5 times with 50:50 acetonitrile/methanol. The hexane phase containing the product was evaporated under vacuum to yield a yellow oil. <sup>1</sup>H-NMR was used to characterize the final product.

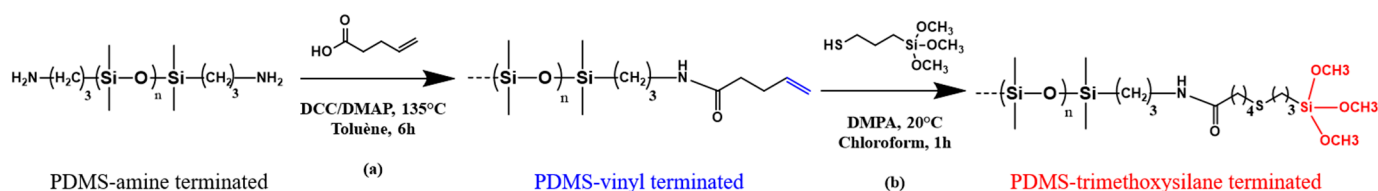


**Figure 1.** Synthetic pathway of modification of polymers with crosslinkable groups. (a) Steglich esterification to obtain vinyl-terminated PDMS (PDMS-V-MW). (b) Thiol-ene coupling to obtain trimethoxysilane-terminated PDMS (PDMS-TMS-MW).

#### 2.2.2. PDMS-V-MW Functionalization via Thiol-Ene Reaction: PDMS-TMS-MW

The crosslinkable PDMS-TMS were synthesized via thiol-ene reaction between (3-mercaptopropyl)-trimethoxysilane (HS-TMS) and vinyl-terminated polydimethylsiloxane (PDMS-V) (Figure 1). The PDMS-V, the HS-TMS (1:2.2 molar ratio), and a catalytic amount of 2,2-dimethoxy-2-phenylacetophenone were dissolved in chloroform. The thiol-ene reaction occurred at room temperature under UV at 365 nm for 1 h. The crude polymer was

purified by solvent extraction with hexane/acetone. After purification the products were analyzed using  $^1\text{H}$  NMR.

### 2.3. Coating Preparation

To evaluate the impact of PDMS molecular weight on antibioadhesion and physico-chemical properties, the coating solutions were applied to glass or PVC slides. The hydrophobic silicone-based coatings were obtained via self-condensation of trimethoxysilane-terminated polydimethylsiloxane with various molecular weights. The crosslinkable PDMS-TMS and the zinc catalyst (2.5 wt%) were dissolved in chloroform (1:1 wt). The mixture was homogenized for 5 min with a lab shaker. The preparation in liquid state was applied immediately after mixing onto a glass slide and a PVC surface by drop deposition. Glass substrates were used only for surface characterizations during laboratory assays, and PVC plates for marine field tests, because PVC surfaces are more suitable for our primers. The coatings were cured at room temperature for 5 days, then dried under vacuum at 50 °C for 48 h. Transparent coatings were named as follows: PDMS-0.8K (800 g·mol<sup>-1</sup>), PDMS-2.5K (2500 g·mol<sup>-1</sup>), PDMS-4K (4010 g·mol<sup>-1</sup>), PDMS-6K (6000 g·mol<sup>-1</sup>), and **PDMS-10K** (9400 g·mol<sup>-1</sup>). The final film thickness measured via an Elcometer 456 (Elcometer®, La Chappelle Saint Mesmin, France), was approximately 200 µm.

### 2.4. Characterization

#### 2.4.1. Proton Nuclear Magnetic Resonance Spectroscopy

The  $^1\text{H}$  NMR spectra of the modified polymers were recorded at room temperature on a Bruker (Billerica, MA, USA) 500 MHz spectrometer using deuterated chloroform ( $\text{CDCl}_3$ ) as the standard. Peak shifts were calibrated from residual solvent peaks. The  $^1\text{H}$  NMR of Steglich esterification was monitored via the following peak shift  $\delta$  (ppm): apparition of allyl protons peak at 6–5 ppm (m, 2 H,  $\text{CH}_2\text{-CH}=\text{CH}_2$ ) and 5–4 ppm (m, 4 H,  $\text{CH}_2\text{-CH}=\text{CH}_2$ ), and the shift of the proton close to amide function, 3 ppm (m, 4 H,  $\text{CH}_2\text{-NH-CO-CH}_2$ ). The  $^1\text{H}$  NMR of thiol-ene coupling was distinguished by the decrease in allyl protons peaks and the apparition of trimethoxy groups at 3.5 ppm (s, 9 H,  $\text{Si}(\text{OCH}_3)_3$ ).

#### 2.4.2. Gel Permeation Chromatography

GPC chromatograms were measured using an Agilent Technologies (Santa Clara, CA, USA) 1200 Infinity II chromatography containing an isocratic pump, a column oven at 35 °C and a RID detector equipped with a Varian 410 autosampler. Two Viscotek T2000 and T3000 series columns (org GPC/SEC 300 × 8 mm) and a guard column (Org Guard, 10 × 4.6 mm) from Malvern (Malvern Panalytical, Palaiseau, France) were used. Polystyrene standards (PolyCAL UCS-PS) from Malvern were used for the molecular weight calibration curve. The samples were dissolved in HiPerSolv CHROMANORM® HPLC grade THF (VWR International, Radnor, PE, USA) and filtered through 0.45 µm PTFE syringe filters. The filtrate was then analyzed at a flow rate of 1 mL·min<sup>-1</sup>. Data were collected and analyzed using Cirrus Software (version 2.0) from Aligent technologies.

#### 2.4.3. Soxhlet Extraction

To determine the efficiency of the crosslinking, the number of uncrosslinking materials in the coating was determined via Soxhlet extraction. The film was removed from the glass slides and extracted with chloroform in a Soxhlet device for 24 h at 90 °C under reflux. The weight loss was then calculated and corresponded to the difference between the extracted and unextracted weight divided by the unextracted weight, as follows:

$$\text{Weight loss}(\%) = \frac{W_0 - W_{ex}}{W_0}$$

### 2.5. Surface Characterization

Coatings were observed using a Scanning Electron Microscope JEOL—IT500 HR SED (Secondary Electron Detector) (Tokyo, Japan). Samples were metallized with gold to obtain a conductive material. Each sample was scanned, and a screenshot of the most representative global topography was taken (magnification 2000×). For all investigations, the beam energy was 10 kV.

Static contact angle measurement was performed using a Digidrop GBX (Dublin, Ireland) system at room temperature (20 °C). Three replicates of deionized water, formamide, and methylene iodide contact angles were measured for each sample. For each replicate three coated surfaces were analyzed. The static contact angle ( $\theta$ ) was measured at five different locations for each coated surface with a 3  $\mu$ L droplet after 3 s of stabilization. The indicated values were an average measured on different coated surfaces. Surface energy for each sample was calculated via the Owens–Wendt method [16] using the average of the static contact angle measurement. Both the dispersive and polar components were assessed ( $\gamma_S = \gamma_S^D + \gamma_S^P$ ). Measurements were performed on PDMS samples after curing.

Atomic force microscopy (AFM) was used to study the surface topography of the coatings. A Multimode 8 AFM instrument equipped with a NanoScope V controller (Bruker, Santa Barbara, CA, USA) was used. Images were recorded using the ScanAsyst<sup>®</sup> mode and the Peak Force Quantitative Nanomechanical Mode (PFQNM<sup>®</sup>). Topographical images were recorded on a sample area of 1  $\mu$ m  $\times$  1  $\mu$ m in the ScanAsyst under ambient conditions using a ScanAsyst-Air cantilever (resonance frequency of 70 KHz, spring constant of  $\sim$ 0.4 N $\cdot$ m<sup>-1</sup> and tip radius of 10 nm) at a scan rate velocity below 2  $\mu$ m $\cdot$ s<sup>-1</sup>. Topographic images were analyzed using NanoScope Analysis software version 1.8. For each coated surface, images were recorded at varying locations. PFQNM was used for determining the nanomechanical properties of the different samples. The piezo in PFQNM was oscillating vertically at a frequency of 2 KHz and an amplitude of 150 nm. With a constant force that was maintained by the peak force feedback loop, a force–distance curve was recorded at each pixel while the piezo scanned the samples beneath the tip (scan velocity 2 mm $\cdot$ s<sup>-1</sup>). The thermal tuning approach for the ScanAsyst tip (spring constant of 0.34 N $\cdot$ m<sup>-1</sup>) was used to calibrate the cantilever's spring constant. The linear portion of an average of 10 forced resistance curves generated by ramping the tips onto a Sapphire surface was used to calculate their deflection sensitivity. The tip radius was calibrated using the relative technique based on reference samples (PFQNM SPM kit 12 M, Bruker), with a PDMS standard of 2.5 MPa for the ScanAsyst tip. The peak force setpoints for the PDMS surfaces were commonly set at 20 pN based on these calibration standards. All measurements were made in natural lighting. Real-time analysis of the force curves from each contact between the tip and the sample produced a nanomechanical map in addition to a topographical image. The modulus was calculated according to the Derjaguin–Muller–Toporov (DMT) model (i.e., a Hertz model including the effect of adhesion without any change in the contact area) [17]. All AFM data analysis and image processing were made using NanoScope software version 1.8.

### 2.6. Marine Field Test

The samples were coated on PVC plates (12 cm  $\times$  6 cm) first covered by a primer and a tie-coat, both supplied by our industrial partner, to ensure good adhesion of the coatings to the panels during immersion. The samples were dried at room temperature for 10 days before immersion. The coatings were immersed vertically in the Atlantic Ocean near Lorient. In order to study the influence of solar irradiation on the development of organisms, the samples were coated on both sides of the PVC surface: one exposed to radiation from sunlight, the other to shade. The antibioadhesion efficiency was evaluated in static conditions over 12 months from June 2022 to July 2023. The samples were removed from the water once a week and photographed before being re-immersed. The pictures of different coatings were compared to evaluate their antibioadhesion efficiency.



### 3. Results and Discussion

#### 3.1. Modification of PDMS Polymers

The preparation of PDMS with crosslinking groups was achieved using thiol-ene click chemistry to attach the trimethoxysilane group to the PDMS vinyl-end group. For the amine-terminated PDMS (PDMS-N2.5K), the end group was first modified via Steglich esterification. This reaction allowed the formation of an amide (Figure 1). The modified crosslinkable PDMS were then characterized using  $^1\text{H-NMR}$  and GPC to evaluate the structure and the molecular weight.

The dry product of PDMS-V2.5K was analyzed using  $^1\text{H NMR}$ . The shift of the proton H4 assigned to the proton close to amide group from 2.7 ppm to 3.4 ppm confirmed the transformation of the amine group into an amide group (Figure 2), thus the formation of symmetric vinyl-terminated PDMS. The yield calculated from its relative intensity was close to 90%. The presence of a vinyl peak at 5.0–5.25 ppm and 5.7–6.0 ppm on the  $^1\text{H NMR}$  spectra, corresponding to H<sub>8</sub> and H<sub>9</sub>, showed the success of the Steglich modification.

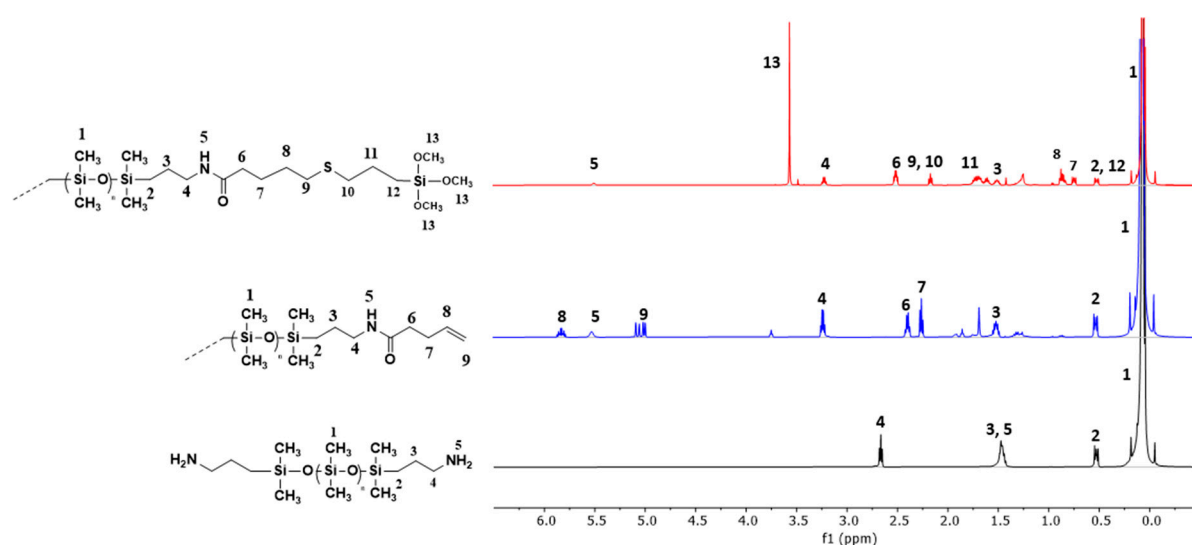


**Figure 2.**  $^1\text{H NMR}$  spectra of PDMS polymers after modification and purification. (Black) amine-terminated PDMS. (Blue) vinyl-terminated PDMS after Steglich esterification. (Red) trimethoxysilane-terminated PDMS after thiol-ene reaction.

The vinyl-terminated polymers (PDMS-V0.8K, PDMS-V2.5K, PDMS-V6K, and PDMS-V10K) were analyzed using  $^1\text{H NMR}$  after thiol-ene reaction. The  $^1\text{H NMR}$  spectra showed a decrease in vinyl proton peaks. In addition, the apparition of methoxy after purification confirmed the coupling between the vinyl group and the thiol trimethoxysilane group, thus the formation of symmetric trimethoxysilane-terminated PDMS (Figure 2). The yield calculated from the proton relative intensities of the trimethoxysilane group was >90%. The molecular weight and polydispersity of modified PDMS after thiol-ene were measured via GPC (Table 1). The molecular weights calculated via GPC were different from the values obtained using  $^1\text{H NMR}$ . This could be explained by the use of polystyrene standards to calculate molecular weight. Also, the observed polydispersity values suggested a heterogeneity of the samples in terms of size. This could be attributed to the reactivity of trimethoxysilane functions, which are sensitive to moisture. They may start to react during GPC analysis, leading to an increase in macromolecule chain size.

**Table 1.** Characterization of modified polymers.

Commercial Polymers	Theoretical Molar Masses $\text{g}\cdot\text{mol}^{-1}$	Modified Polymers	Molar Masses by $^1\text{H}$ NMR $(\text{g}\cdot\text{mol}^{-1})^a$	Molar Masses by SEC $(\text{g}\cdot\text{mol}^{-1})^b$	$\bar{M}_w$
PDMS-V0.8K	800	PDMS-TMS0.8K	858	1341	1.83
PDMS-N2.5K	2500	PDMS-TMS2.5K	2775	4404	2.18
PDMS-TMS4K	4010	-	3774	4775	2.06
PDMS-V6K	6000	PDMS-TMS6K	5164	7173	3.14
PDMS-V10K	9400	PDMS-TMS10K	9021	11,720	2.78

<sup>a</sup> Calculated with relative intensities of peak of PDMS at 0.04 ppm. <sup>b</sup> In THF as eluent and with polystyrene standard.

### 3.2. Preparation of PDMS Coating

The trimethoxysilane-terminated PDMS (PDMS-TMS0.8K, PDMS-TMS2.5K, PDMS-TMS4K, PDMS-TMS6K and PDMS-TMS10K) were solubilized in chloroform with the catalyst, and homogenized with a vortex for 5 min to ensure good homogenization. The proportions of catalyst and solvent were kept consistent. After the curing process, the coatings obtained were colorless, with a smooth surface and good adhesion on a glass surface. All formulations had good film-forming properties except for the lowest molar mass, PDMS-0.8K, which showed cracks; the coating was too brittle and cracked during the curing stage.

To demonstrate the complete crosslinking of PDMS films, a Soxhlet extraction test was carried out on each sample. The quantitative residue of uncrosslinking chains was evaluated via mass loss calculations after Soxhlet extraction. Figure 3 shows the weight loss of each coating according to molecular weight. The calculated weight loss was less than 4 wt% for all formulations, which showed an excellent crosslinking efficiency. Similar results were observed by Drebezghova et al. for PDMS-based coatings cured via a hydrosilylation reaction [18]. PDMS-2.5K showed a higher mass loss compared to the other coatings. The PDMS-2.5K polymer was obtained after a two-synthesis step which reduced the overall yield compared with other polymers that were obtained in one step. The higher ratio of PDMS macromolecules without a TMS end-group could explain the higher mass loss during Soxhlet analysis. In another study, where a sol-gel reaction occurred between a silanol and a triethoxysilane, lower weight loss was observed ( $\approx 1$  wt%) [19]. In such a network, triethoxysilane-terminated PDMS was used as a crosslinker which allowed easier and more significant crosslinking compared to self-condensation, leading to fewer free chains. Moreover, uncrosslinked chains were not the only materials that could be released from the films; the catalyst was soluble in chloroform and could be extracted. It was most important to show there were no significant free polymer chains in the network system, because their presence could impact surface properties such as contact angle, atomic composition, AFM Young's modulus, and bacterial retention, as shown in Drebezghova et al.'s recent study [18].

### 3.3. Surface Properties of PDMS Coatings

After the curing process, the surface of PDMS coatings were investigated via SEM, contact angle measurements, and AFM. Scanning electron microscopy was employed to assess the surface morphology of the PDMS coatings on the micrometer scale. Images obtained via SEM for all coatings were similar and showed PDMS elastomer surface morphology as seen in supplementary data (Figure S1). SEM images showed homogeneous surfaces with no aggregates. These results were in agreement with the literature. Gillet et al. observed the same result for PDMS coatings obtained via a condensation process [15]. The different PDMS polymers showed similar SEM morphologies, suggesting that at this scale, the distance between crosslinking nodes, hence the molecular weight, did not affect the morphology of the PDMS network.



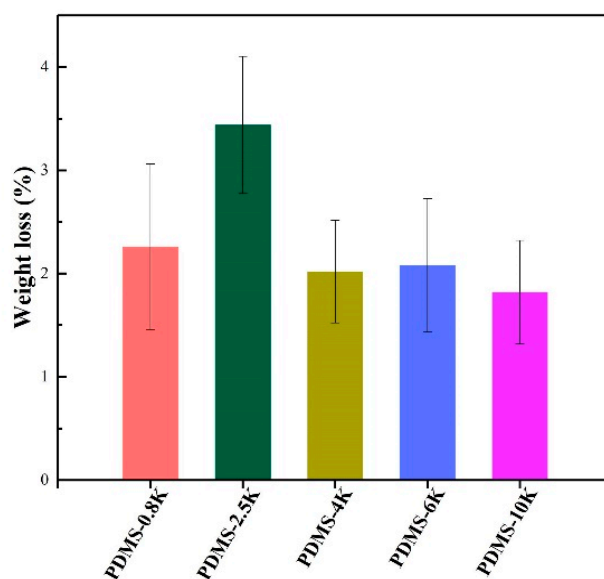


**Figure 3.** Observed weight loss after Soxhlet extractions of PDMS-based coatings.

For a better observation of the network morphology of PDMS-based coatings, atomic force microscopy (AFM) was performed in a dry state in ambient conditions in air, to assess surface topography and roughness. The smoothness of an antibioadhesion coating seems to be an important parameter to avoid bioadhesion: many studies report that a decrease in surface roughness can be related to a reduction in bacterial adhesion [20,21]. The surface topography of coatings at different molecular weights were examined at nanometric scale ( $0.25 \mu\text{m}^2$ ) (Figure 4), and analysis of image sections enabled the determination of the roughness mean square (RMS). The RMS values of the coatings are represented in Figure 5. PDMS surfaces showed a very smooth surface with low RMS values around 2 nm to 6 nm. All PDMS coatings exhibit a typical mesh-like network structure as described by Drebezghova et al. [22]. The low roughness of the coatings was not surprising according to the literature [22,23]. The RMS values of the films were between 1 and 6 nm, with a slight increase of the RMS when increasing molecular weight of the PDMS, indicating the molecular weight could impact the surface roughness of coatings. The coating with the higher molecular weight, PDMS-10K, presented domains with higher RMS values compared to PDMS-2.5K, for example. To the best of our knowledge, there is no study reported in the literature regarding the correlation between the molecular weight of polymers and the RMS values of crosslinked PDMS. In our study, further experiments to interpret this variation, such as precise control of the crosslinking rate of the film, were necessary. We could nonetheless hypothesize that the structural organization of the polymer chain at the surface of the film may be modified by the length of the polymer, between crosslinked points, to generate local z variation in the film surface topography.

Surface elasticity of coatings can be measured using a contact mechanics model (the hertz model) using AFM. Young's moduli of PDMS coatings were found to be around 0.3–3.2 MPa. Variation depending on the chain size of the different polymers was observed. PDMS-0.8K with the lowest molecular weight seems to have a higher value of elastic modulus ( $3.20 \pm 0.01$  MPa) compared to other coatings. PDMS-2.5K ( $0.58 \pm 0.01$  MPa), PDMS-4K ( $1.64 \pm 0.08$  MPa), PDMS-6K ( $0.44 \pm 0.03$  MPa) and PDMS-10K ( $0.34 \pm 0.11$  MPa) appear to be in the same range. Therefore, the molecular weight seems to affect elastic moduli, which is only relevant for coatings with significantly different chain sizes. For example, PDMS-0.8K has an elastic modulus nine times higher than that of PDMS-10K. However, these values were in good accordance with previous studies, as elastic moduli for fouling release coatings are typically ranged between 0.2 and 9 MPa [3,23–25]. In their recent study, similar results were observed by Sun et al. [26]. They observed that when the crosslinking density of the polymeric network of PDMS decreases, Young's

modulus consequently decreases from 8.90 to 2.99 MPa. It was assumed that the lower the molecular weight of PDMS, the smaller the network size [27]. It appears that when a higher molecular weight was used, the distance between the crosslinking point increased, leading to lower Young's modulus compared to the PDMS-0.8K ( $3.20 \pm 0.01$  MPa) and PDMS-10K ( $0.34 \pm 0.11$  MPa).

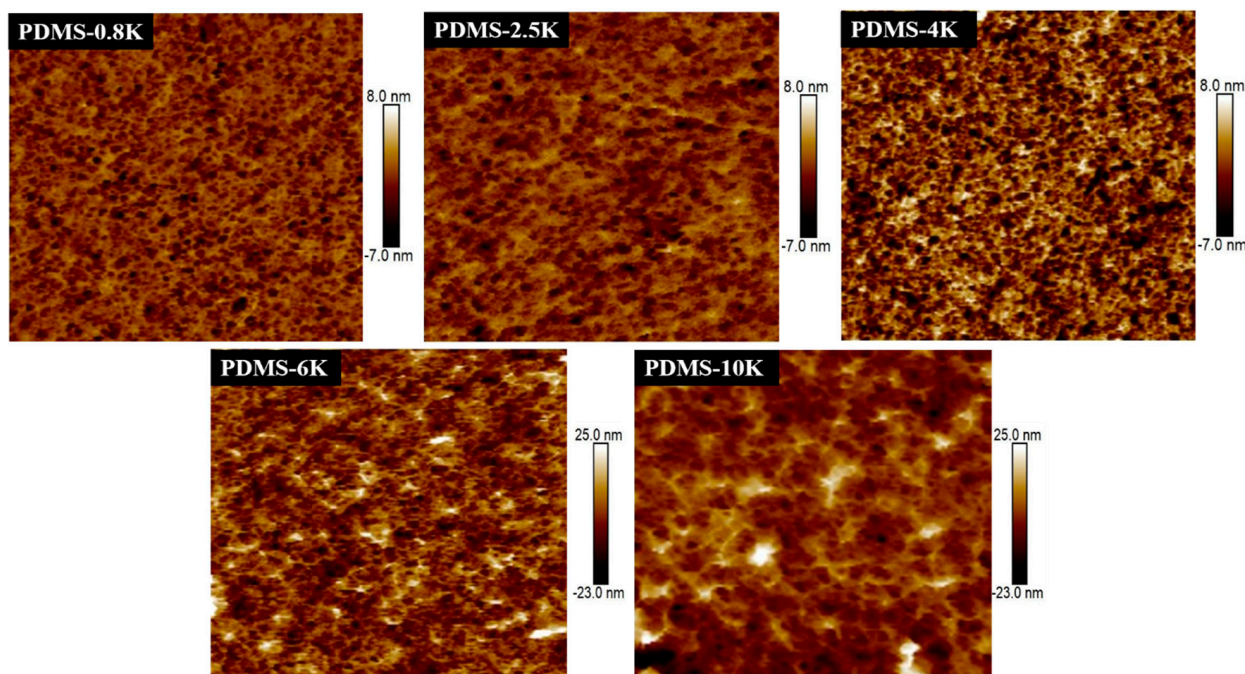


**Figure 4.** Representative AFM height images ( $0.5 \mu\text{m} \times 0.5 \mu\text{m}$ ) showing topography of PDMS coating of PDMS-0.8K, PDMS-2.5K, PDMS-4K, PDMS-6K and PDMS-10K.

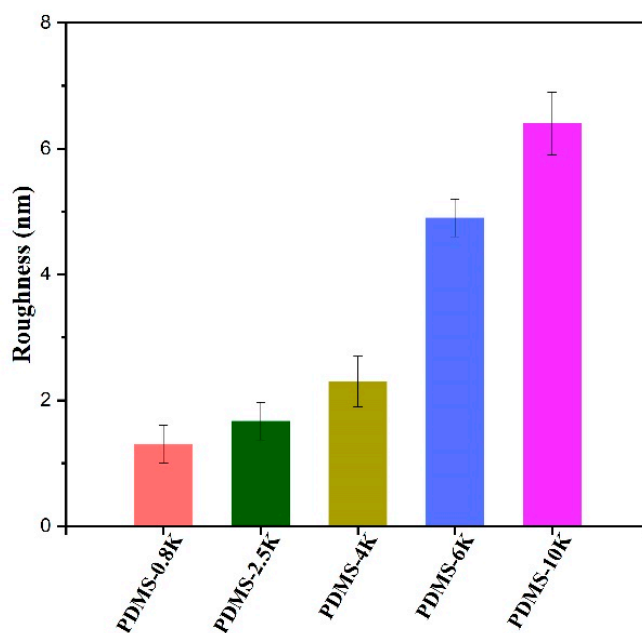


**Figure 5.** RMS values of PDMS-based coating obtained via AFM.

Contact angle measurement was used to examine the wetting properties and surface free energy depending on the molecular weight of PDMS. The contact angle was measured in static conditions. Figure 6a shows the results of contact angle measurements for three

solvents. Unsurprisingly, all PDMS coatings showed a hydrophobic character, with high contact angle values comparable to what is found in the literature ( $\theta_{\text{water}} \geq 100^\circ$ ). PDMS-2.5K was slightly more hydrophobic than other PDMS-based coatings ( $\theta_{\text{water}} = 108^\circ$ ). There was no change in hydrophobicity as function of molecular weight of the PDMS coatings. Figure 6b illustrates the surface energy (SE) calculated from the water contact angle (WCA), methylene iodide (MICA), and formamide (FCA) values using the Owen–Wendt method. Surface energies of the PDMS coatings were between 18 and 23 mN/m. Gevaux et al. found similar values for the surface energy of PDMS coatings ( $\gamma_s \approx 18 \text{ mN/m}$ ) [28]. Lower surface energy was observed for the PDMS-0.8K coating with low molecular weight. Despite this, there was no correlation between surface energy and molecular weight. This implies that there is no chemical change at the surface of the coating depending on the size of the macromolecules at this scale.

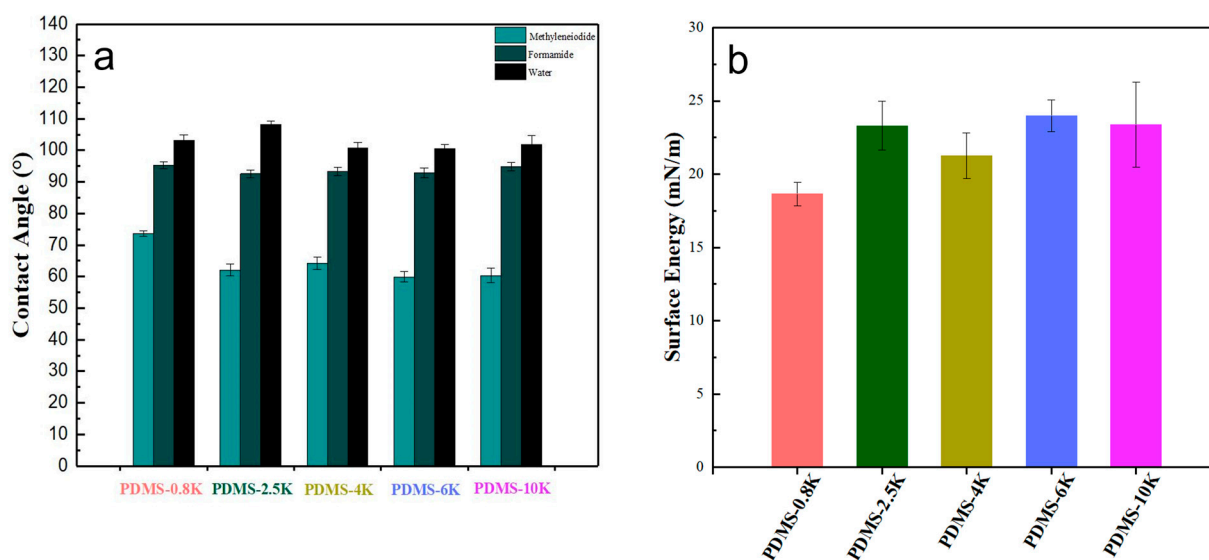


**Figure 6.** Contact angle measurement with different solvents (a) and surface energy calculation (b) of PDMS-based coatings.

### 3.4. Marine Field Test

The evaluation of the antibioadhesion and self-cleaning performances of PDMS coatings was carried using in situ experiments. Coated PVC-panels were immersed in the Atlantic Ocean in static conditions for 12 months. It is important to note that they were immersed at the beginning of the summer season, which is the harshest season for fouling development. In temperate climates, seasonality has a significant impact on the colonization and success of biofouling communities; less fouling develops in the winter as a result of the lower seawater temperature and solar radiation intensity [29,30]. Higher fouling pressure results from rising nutrient levels and seawater temperature from spring to late summer. In this present work, the impact of solar radiation on the fouling communities was also evaluated by observing the proliferation of macrofouling on different immersed surfaces. Two faces of coated surfaces were observed: one face exposed to the sun and the other not. The antibioadhesion efficiency of the coatings was assessed by comparison with an uncoated PVC surface, as a control.

Firstly, the images were observed after 5 months of immersion. The different images in Figure 7 show the antibioadhesion efficiency depending on the PDMS molecular weight and solar radiation after 5 months. As expected, the control surfaces were quickly fouled by macroorganisms, indicating the suitability of the chosen immersion site. Different types of marine fouling adhered depending on the solar radiation. Surfaces exposed to solar radiation were mostly covered by brown slime and algae. However, with no solar radiation surfaces were mainly colonized by other hard fouling organisms: barnacles,

sponges, or bryozoans. After five months in seawater, all samples were colonized, but covered less than the control. The best antibioadhesion efficiency for panels under solar exposition was observed for PDMS-2.5K and PDMS-4K. For panels immersed in the absence of solar exposition the PDMS-2.5K did not exhibit the same AF efficiency. The self-cleaning properties of PDMS-6K were observed after three months, as organisms were removed during immersion without any intervention, indicating their weaker adhesion to the surface. The same property was observed for PDMS-4K. An image of this phenomenon can be seen in the supplementary data (Figure S2). The efficiency of fouling release coatings is estimated by the strength of adhesion of settled fouling organisms [4,5,31]. Hence, PDMS-4K and PDMS-6K seemed to display a fouling release efficiency because of their self-cleaning capacity.

The antibioadhesion efficiency of all PDMS-based coatings after 12 months can be seen in Figure 8. After 12 months of immersion, the PDMS-6K sample started to lose its antibioadhesion efficiency while the PDMS-2.5K and PDMS-4K coatings still exhibited the best efficiency under solar radiation, being only covered by a brown film of algae. The PDMS samples with the highest molecular weight, PDMS-6K and PDMS-10K, exhibited less antibioadhesion efficiency. The poor performance of the lowest molecular weight, PDMS-0.8K, could be attributed to its poor film-forming properties. The coating exhibited cracks before immersion which created heterogeneity on the surface and anchor points for the biofouling. In the absence of solar exposition, all the surfaces were completely covered after 12 months of immersion, with no significant difference between the PDMS surfaces (Figure 8). However, the biovolume of fouling settled on surface was found to be greatly lower after 12 months compared to 5 months. These results showed that in terms of efficiency, two groups of molecular weight could be distinguished, with better efficiency for lower molecular weight. It is difficult here to make a correlation between surface energy and the settlement. Different reviews reported that lower surface energy contributed to decreased bacterial settlement. In the present case, no significant change was observed for PDMS coatings in terms of surface energy measurement, and the observed surface energy values were consistent with the minimum range defined by Baier [4] for best fouling release properties. Despite that, differences in antibioadhesion efficiency have been observed. It's also known that surface roughness plays an important role in the adhesion process: lower surface roughness can reduce bacterial adhesion [20]. However, this observation remains controversial, as in certain studies the opposite result has been observed. In fact, Liu et al. studied the adhesion of *Escherichia coli* (Gram-negative) and *Staphylococcus aureus* (Gram-positive) on nanostructured PDMS surfaces, and found that increasing the nanoscale roughness on PDMS surfaces alone can inhibit bacterial adhesion and growth for both bacteria [32]. In a recent review on the effect of surface structure on bacterial adhesion [33], Yang et al. plotted the adhesion of cells as a function of the roughness parameters (RMS or Ra) for various substrates. Above a critical Ra value, estimated to be approximately 6 nm, their plot demonstrated a generally positive correlation between the number of cells adsorbed on the surface and the roughness, while a negative, or no correlation, is noted below the Ra value. They concluded that microscale roughness generally encourages bacterial adhesion and nanoscale roughness provides the best antibioadhesion efficiency [33].

In our work, we can see that our films have a nanometer size RMS (1–6 nm), even if a small variation in nanoscale roughness with the molecular weight can be observed. The nanometer RMS of our films (below the critical Ra value defined by Yang et al. [33]) is thus likely to have no impact on the adhesion of micro or macroorganisms, and this parameter is probably not determinant in our experiments, as revealed by the bioadhesion test in a real marine environment. Indeed, low long-term efficiency was observed for the PDMS-6K and PDMS-10K coatings, which presented high roughness at the nanoscale as compared with the PDMS-2.5K and PDMS-4K (low surface roughness), which showed better efficiency. It appears that the RMS parameter alone cannot explain this difference,



but that other parameters should be considered, such as the mechanical properties, or more local organizational parameters such as the glass temperature  $T_g$  or chain end.



Figure 7. Macrofouling development observed on PDMS-based coatings (4 cm × 3 cm).

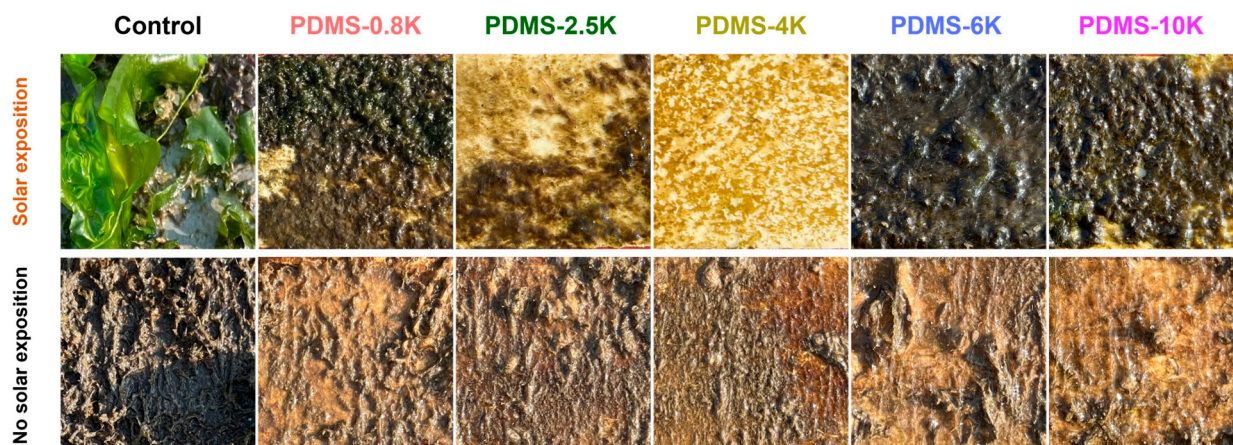


**Figure 8.** Marine field test of PDMS-based coatings after 12 months in Lorient Bay (5 cm × 5 cm).

Stiffness was found to be another parameter which can affect bacterial adhesion in different studies [24,34], even if it is less well understood. Song et al. reported that a Young's modulus of PDMS coatings ranging between 0.1 and 2.6 MPa not only affected the attachment of bacteria, but also the morphology and antibiotic susceptibility of attached cells [24]. More biofilm growth was observed on a soft PDMS surface (0.1 MPa) than on a stiff PDMS (2.6 MPa). Similar results were reported by Valentin et al. on *Escherichia coli* adhesion under dynamic condition [34]. It should be noted that the coatings obtained in these previous studies were prepared in the presence of precursors. The PDMS-based coatings prepared in this work were obtained via a self-condensation process, by varying the molecular weight and some network properties. Our hypothesis is that in PDMS coatings with higher molecular weight, the network is less dense due to the long distance between crosslinking nodes compared to a network with a short chain. For example, this spacing between meshes could change the mechanical properties. However, the preliminary studies on PDMS surfaces prepared here showed surface stiffness between 0.3 and 3.2 MPa, with no correlation with the molecular weight. Another property impacted by chain size is the chain mobility between cross-linking nodes and the associated free volume. Indeed, in a network of long chains, there is more free volume which could lead to different interactions with organisms.

Finally hydrodynamic forces and shear stress may be responsible of the release of organisms when it concerns a fouling release coating [31]. In these conditions, the smoother the surface, the easier it is to release the organisms [35]. In our study, except for sample PDMS-0.8K, the samples with lower surface roughness showed better antibioadhesion activity than the samples with higher nanoscale surface roughness. Nevertheless, further studies are needed to understand the network structure related to the molecular weight. It is important to note that due to the complexity of the marine environment, other parameters may be relevant during the adhesion process.

#### 4. Conclusions

In this work, we investigated the impact of the molecular weight of PDMS on the antibioadhesion efficiency of corresponding coatings. By varying the molecular weight, we prepared five PDMS-based coatings via a condensation process. Soxhlet extraction results confirmed that the PDMS networks were well crosslinked and showed there was no significant free polymer chains. Homogenous PDMS coatings were obtained and all PDMS-based coatings showed a low surface energy, low elastic modulus and low surface roughness, making them suitable for marine applications. From contact angle measurement, no correlation between the molecular weight and the surface energy was observed. Moreover, changes in surface roughness were observed via AFM, with the RMS increasing with the molecular weight due to the growth of network free volume. Overall, PDMS-based surfaces showed good antibioadhesion activity and self-cleaning



abilities compared to the control after 12 months. The best antibioadhesion efficiency was obtained for coatings with an Mn between 2 and 4 kg·mol<sup>-1</sup>. This result is explained by the chain mobility in the network. In situ immersion results showed that in the presence or absence of solar radiation, different communities of organisms adhere on the surface, leading to differences in antibioadhesion performance. This work provides evidence that some network properties, depending on the size of the polymer chains, contribute to antibioadhesion and self-cleaning efficiencies. However, further characterization is needed to focus on the crosslinking density, the chain mobility, and the network structure of PDMS-based coatings.

**Supplementary Materials:** The following supporting information can be downloaded at <https://www.mdpi.com/article/10.3390/coatings14010149/s1>, Figure S1: SEM images of PDMS-based coating as function of molar masses: (a) P PDMS-0.8K, (b) PDMS-2.5K, (c) PDMS-4K, (d) PDMS-6K, (e) PDMS-10K; Figure S2: Attachment of macrofouling on sample PDMS-6K over time with no solar radiation.

**Author Contributions:** Conceptualization, M.A.B. and F.A.; methodology, M.A.B., E.B. and F.A.; investigation, M.A.B.; writing—original draft, M.A.B.; review & editing, F.A. and K.R.; resources, M.A.B. and F.A.; funding acquisition, K.R. and I.L.; project administration, F.A. and I.L. Supervision, D.M. All authors have read and agreed to the published version of the manuscript.

**Funding:** This research was funded by Agence Nationale de la Recherche grant number 15-LCV4-0006.

**Institutional Review Board Statement:** Not applicable.

**Informed Consent Statement:** Not applicable.

**Data Availability Statement:** Data are contained within the article and supplementary materials.

**Acknowledgments:** We sincerely thank our industrial partner for the kind gift of some materials. The authors want also to acknowledge Anthony Magueresse for help with SEM images.

**Conflicts of Interest:** The authors declare no conflict of interest.

## References

1. Yebra, D.M.; Kiil, S.; Dam-Johansen, K. Antifouling Technology—Past, Present and Future Steps towards Efficient and Environmentally Friendly Antifouling Coatings. *Prog. Org. Coat.* **2004**, *50*, 75–104. [[CrossRef](#)]
2. Schultz, M.P.; Bendick, J.A.; Holm, E.R.; Hertel, W.M. Economic Impact of Biofouling on a Naval Surface Ship. *Biofouling* **2011**, *27*, 87–98. [[CrossRef](#)] [[PubMed](#)]
3. Lejars, M.; Margailan, A.; Bressy, C. Fouling Release Coatings: A Nontoxic Alternative to Biocidal Antifouling Coatings. *Chem. Rev.* **2012**, *112*, 4347–4390. [[CrossRef](#)] [[PubMed](#)]
4. Baier, R.E. Surface Behaviour of Biomaterials: The Theta Surface for Biocompatibility. *J. Mater. Sci. Mater. Med.* **2006**, *17*, 1057–1062. [[CrossRef](#)] [[PubMed](#)]
5. Chaudhury, M.K.; Finlay, J.A.; Chung, J.Y.; Callow, M.E.; Callow, J.A. The Influence of Elastic Modulus and Thickness on the Release of the Soft-Fouling Green Alga *Ulva linza* (Syn. Enteromorpha Linza) from Poly(Dimethylsiloxane) (PDMS) Model Networks. *Biofouling* **2005**, *21*, 41–48. [[CrossRef](#)] [[PubMed](#)]
6. Kim, J.; Chisholm, B.J.; Bahr, J. Adhesion Study of Silicone Coatings: The Interaction of Thickness, Modulus and Shear Rate on Adhesion Force. *Biofouling* **2007**, *23*, 113–120. [[CrossRef](#)] [[PubMed](#)]
7. Pouget, E.; Tonnar, J.; Lucas, P.; Lacroix-Desmazes, P.; Ganachaud, F.; Boutevin, B. Well-Architected Poly(Dimethylsiloxane)-Containing Copolymers Obtained by Radical Chemistry. *Chem. Rev.* **2010**, *110*, 1233–1277. [[CrossRef](#)]
8. Lampe, W.R.; Moore, A.A.; Hartley, K.R. Marine Foulant Release Coating. U.S. Patent 4861670A, 29 August 1989.
9. Wynne, K.; Swain, G.; Fox, R.; Bullock, S.; Uilk, J. Two Silicone Nontoxic Fouling Release Coatings: Hydrosilation Cured PDMS and CaCO<sub>3</sub> Filled, Ethoxysiloxane Cured RTV11. *Biofouling* **2000**, *16*, 277–288. [[CrossRef](#)]
10. Edward, R. Ship's Hull Coated with Anti-Fouling Silicone Resin and Method of Coating. U.S. Patent 2986474A, 30 May 1961.
11. Truby, K.; Wood, C.; Stein, J.; Cella, J.; Carpenter, J.; Kavanagh, C.; Swain, G.; Wiebe, D.; Lapota, D.; Meyer, A.; et al. Evaluation of the Performance Enhancement of Silicone Biofouling-Release Coatings by Oil Incorporation. *Biofouling* **2000**, *15*, 141–150. [[CrossRef](#)]
12. Qiu, C.; Xiong, W.; Zhang, H.; Zhang, R.; Parkin, I.P.; Wang, S.; Li, L.; Chen, J.; Chen, Z.; Tapa, A.R.; et al. Superhydrophobicity Transfer Effect in Superwetting Coatings for Strengthening Anti-Pollution Flashover Performance. *Prog. Org. Coat.* **2024**, *186*, 107955. [[CrossRef](#)]

13. Stein, J.; Truby, K.; Wood, C.D.; Stein, J.; Gardner, M.; Swain, G.; Kavanagh, C.; Kovach, B.; Schultz, M.; Wiebe, D.; et al. Silicone Foul Release Coatings: Effect of the Interaction of Oil and Coating Functionalities on the Magnitude of Macrofouling Attachment Strengths. *Biofouling* **2003**, *19*, 71–82. [[CrossRef](#)] [[PubMed](#)]
14. Gray, N.L.; Banta, W.C.; Loeb, G.I. Aquatic Biofouling Larvae Respond to Differences in the Mechanical Properties of the Surface on Which They Settle. *Biofouling* **2002**, *18*, 269–273. [[CrossRef](#)]
15. Gillet, G.; Azemar, F.; Faÿ, F.; Réhel, K.; Linossier, I. Non-Leachable Hydrophilic Additives for Amphiphilic Coatings. *Polymers* **2018**, *10*, 445. [[CrossRef](#)] [[PubMed](#)]
16. Owens, D.K.; Wendt, R.C. Estimation of the Surface Free Energy of Polymers. *J. Appl. Polym. Sci.* **1969**, *13*, 1741–1747. [[CrossRef](#)]
17. Derjaguin, B.V.; Muller, V.M.; Toporov, Y.P. Effect of Contact Deformations on the Adhesion of Particles. *J. Colloid Interface Sci.* **1975**, *53*, 314–326. [[CrossRef](#)]
18. Drebezhova, V.; Hakil, F.; Grimaud, R.; Gojzewski, H.; Vancso, G.J.; Nardin, C. Initial Bacterial Retention on Polydimethylsiloxane of Various Stiffnesses: The Relevance of Modulus (Mis)Match. *Colloids Surf. B Biointerfaces* **2022**, *217*, 112709. [[CrossRef](#)]
19. Murthy, R.; Cox, C.D.; Hahn, M.S.; Grunlan, M.A. Protein-Resistant Silicones: Incorporation of Poly(Ethylene Oxide) via Siloxane Tethers. *Biomacromolecules* **2007**, *8*, 3244–3252. [[CrossRef](#)]
20. de Dantas, L.C.M.; da Silva-Neto, J.P.; Dantas, T.S.; Naves, L.Z.; das Neves, F.D.; da Mota, A.S. Bacterial Adhesion and Surface Roughness for Different Clinical Techniques for Acrylic Polymethyl Methacrylate. *Int. J. Dent.* **2016**, *2016*, 8685796. [[CrossRef](#)]
21. Truong, V.K.; Lapovok, R.; Estrin, Y.S.; Rundell, S.; Wang, J.Y.; Fluke, C.J.; Crawford, R.J.; Ivanova, E.P. The Influence of Nano-Scale Surface Roughness on Bacterial Adhesion to Ultrafine-Grained Titanium. *Biomaterials* **2010**, *31*, 3674–3683. [[CrossRef](#)]
22. Drebezhova, V.; Gojzewski, H.; Allal, A.; Hempenius, M.A.; Nardin, C.; Vancso, G.J. Network Mesh Nanostructures in Cross-Linked Poly(Dimethylsiloxane) Visualized by AFM. *Macromol. Chem. Phys.* **2020**, *221*, 2000170. [[CrossRef](#)]
23. Guennec, A.; Brelle, L.; Balnois, E.; Linossier, I.; Renard, E.; Langlois, V.; Faÿ, F.; Chen, G.Q.; Simon-Colin, C.; Vallée-Réhel, K. Antifouling Properties of Amphiphilic Poly(3-Hydroxyalkanoate): An Environmentally-Friendly Coating. *Biofouling* **2021**, *37*, 894–910. [[CrossRef](#)] [[PubMed](#)]
24. Song, F.; Ren, D. Stiffness of Cross-Linked Poly(Dimethylsiloxane) Affects Bacterial Adhesion and Antibiotic Susceptibility of Attached Cells. *Langmuir* **2014**, *30*, 10354–10362. [[CrossRef](#)] [[PubMed](#)]
25. Straub, H.; Bigger, C.M.; Valentin, J.; Abt, D.; Qin, X.-H.; Eberl, L.; Maniura-Weber, K.; Ren, Q. Bacterial Adhesion on Soft Materials: Passive Physicochemical Interactions or Active Bacterial Mechanosensing? *Adv. Healthc. Mater.* **2019**, *8*, 1801323. [[CrossRef](#)] [[PubMed](#)]
26. Sun, J.; Wang, K.; Hao, R.; Zhang, Z.; Feng, Z.; Shi, Z.; Yuan, W.; Jing, Z.; Zhang, L. Disregarded Free Chains Affect Bacterial Adhesion on Cross-Linked Polydimethylsiloxane Surfaces. *ACS Appl. Mater. Interfaces* **2023**, *15*, 36936–36944. [[CrossRef](#)] [[PubMed](#)]
27. Gonzales, R.R.; Kato, N.; Awaji, H.; Matsuyama, H. Development of Polydimethylsiloxane Composite Membrane for Organic Solvent Separation. *Sep. Purif. Technol.* **2022**, *285*, 120369. [[CrossRef](#)]
28. Gevaux, L.; Lejars, M.; Margailan, A.; Bressy, C. Water Erodible Coatings Based on a Hydrolyzable PDMS/Polyester Network. *Mater. Today Commun.* **2018**, *17*, 517–526. [[CrossRef](#)]
29. Dobretsov, S.; Coutinho, R.; Rittschof, D.; Salta, M.; Ragazzola, F.; Hellio, C. The Oceans Are Changing: Impact of Ocean Warming and Acidification on Biofouling Communities. *Biofouling* **2019**, *35*, 585–595. [[CrossRef](#)]
30. Vinagre, P.A.; Simas, T.; Cruz, E.; Pinori, E.; Svenson, J. Marine Biofouling: A European Database for the Marine Renewable Energy Sector. *J. Mar. Sci. Eng.* **2020**, *8*, 495. [[CrossRef](#)]
31. Brady, R.F.; Singer, I.L. Mechanical Factors Favoring Release from Fouling Release Coatings. *Biofouling* **2000**, *15*, 73–81. [[CrossRef](#)]
32. Liu, L.; Ercan, B.; Sun, L.; Ziemer, K.S.; Webster, T.J. Understanding the Role of Polymer Surface Nanoscale Topography on Inhibiting Bacteria Adhesion and Growth. *ACS Biomater. Sci. Eng.* **2016**, *2*, 122–130. [[CrossRef](#)]
33. Yang, K.; Shi, J.; Wang, L.; Chen, Y.; Liang, C.; Yang, L.; Wang, L.-N. Bacterial Anti-Adhesion Surface Design: Surface Patterning, Roughness and Wettability: A Review. *J. Mater. Sci. Technol.* **2022**, *99*, 82–100. [[CrossRef](#)]
34. Valentin, J.D.P.; Qin, X.-H.; Fessele, C.; Straub, H.; van der Mei, H.C.; Buhmann, M.T.; Maniura-Weber, K.; Ren, Q. Substrate Viscosity Plays an Important Role in Bacterial Adhesion under Fluid Flow. *J. Colloid Interface Sci.* **2019**, *552*, 247–257. [[CrossRef](#)] [[PubMed](#)]
35. Azemar, F.; Faÿ, F.; Réhel, K.; Linossier, I. Ecofriendly Silicon-Poly(Lactic Acid) Hybrid Antifouling Coatings. *Prog. Org. Coat.* **2020**, *148*, 105841. [[CrossRef](#)]

**Disclaimer/Publisher's Note:** The statements, opinions and data contained in all publications are solely those of the individual author(s) and contributor(s) and not of MDPI and/or the editor(s). MDPI and/or the editor(s) disclaim responsibility for any injury to people or property resulting from any ideas, methods, instructions or products referred to in the content.